A novel free-standing polymeric composite membrane for osmotic energy generation applications

Dan Li[1], TaiKang Ou[1], Qiang Fu[1,2*], Dian-sen Li[3], ZeMin Liu[1], Youyi Sun[1*]

[1] *School of materials science and technology, North University of China, Taiyuan 030051, P.R. China.*

[2] *School of Civil and Environmental Engineering, University of Technology Sydney, Ultimo NSW 2007, Australia.*

[3] *Key Laboratory of Bio-Inspired Smart Interfacial Science and Technology, Ministry of Education, School of Chemistry, Beijing University of Aeronautics and Astronautics, Beijing 100191.*

Abstract: A novel free-standing polymeric composite membrane was developed to simultaneously achieve high energy density and mechanical robustness for osmotic energy generation. The composite membrane is composed of a poly(vinyl alcohol) (PVA) gel down layer and a thin graphene/sulfonated poly(ether ether ketone) (SPEEK) top layer. The PVA layer offers excellent mechanical stability and flexibility and high water permeability, and the SPEEK think film allows cations to pass through by diffusion. As a result, the composite membrane manages to achieve a high power density of ca. 5.89W/m^2 under a salinity gradient of 50 (0.5 M|0.01 M, NaCl). Furthermore, the energy generation device can maintain the high power output for 4 days or under 300P pressure, indicating excellent long-term stability and mechanical durability. The excellent comprehensive performance is attributed to that down PVA gel and top thin graphene/SPEEK layer both exhibit good ion transport behavior, ion selectivity and membrane stability in saline solution. The work provides a new strategy to design and prepare high-performance membrane for energy harvesting devices.

Key words: Graphene/SPEEK, PVA gel, free-standing, energy conversion, mechanical robustness.

Corresponding authors: YY Sun and Q Fu;

E-mail address: syyi@pku.edu.cn (YY Sun) and qiang.fu@uts.edu.au (Q Fu)

1. Introduction

The use of fossil fuels is arguably one of the major causes of current climate change, altering Earth's ecosystems and causing a series of environmental problems[1]. Since nuclear power facing negative public opinion, researchers are turning their attention to develop renewable and sustainable energy sources that could be safe, reproducible and ecological, such as solar, wind and hydro power[2, 3]. During last decades, the osmotic energy generation (*aka.* blue energy or salinity gradient energy) is considered an environmental friendly and low-carbon technology for sustainable power generation[4-6]. Driven by the Gibbs free energy of high concentration seawater and freshwater mixing, the counter ions preferentially pass through the ion-selective channels within the semipermeable membrane, thereby directly generating electricity[7]. From above respect, the membrane properties, such as water permeability, ion transport behavior, ion selectivity and membrane stability in saline solution are the keys to osmotic energy generation technology.

Generally, the membrane is composed of porous down layer and a thin top layer[8]. The porous down layer mainly acts as supporting substrate, providing good water permeability and good membrane stability, such as porous polymer film[9], porous anodic aluminum oxide (AAO)[10-11], mesoporous carbon[12] and silica membranes[13, 14]. The thin top layer is based on polymer, carbon or other inorganic materials, which acts as ion transporting and ion selective layer[2]. Although these inorganic rigid supporting substrate exhibit high water permeability and ion transport behavior, yet, it also show low ion selectivity, leading to a relatively low power density (< 5.0W m^{-2}). Furthermore, compared with these down and top inorganic rigid layer, polymeric layer can be easily assembled into energy harvesting devices due to high processability and high flexibility. So, recently, all-polymeric membrane is more promising for application energy harvesting devices. For example, Jiang et al reported an organic heterogeneous membrane composed of one layer of functional polyelectrolyte hydrogel membrane and one layer of supporting porous aramid nanofiber (ANF) membrane by a sequential blade-casting method[9]. The resulting membrane achieved a power density of 5.06 W m^{-2}. Zhang et al reported the fabrication of a composite membrane composed of a porous PET substrate and a top layer made from polystyrene-*b*-poly(4-vinylpyridine) (PS-*b*-P4VP). The maximum power output on external electrical load is as high as 0.35 W m^{-2}[15]. Using the same substrate, Xu et al employed TEMPO oxidized cellulose nanofibers to prepare the top layer. The resulting membrane achieved a power density

of 0.96 W m^{-2} [16]. Zhang et al. reported a mechanically strong MXene/Kevlar nanofiber composite membrane for salinity power generation, in which the power density reached *ca.* 4.1 W m^{-2} [17]. These polymeric composite membranes are based on hydrophobic polymer substrate with few pores, indicating a good mechanical stability in saline solution and under water pressure. However, these hydrophobic polymer substrates exhibit low water permeability and ion transport behavior, leading to a low power density. To overcome above problems, two strategy are generally used. Firstly, a free-standing polymeric GO/CNFs composite membrane was developed, in which the substrate was removed. The power density was improved to be 4.19W m^{-2} [18]. Secondly, a hydrophilic polymer substrate (e.g. SPSF) was developed, in which a high power density of *ca.* 7 W m^{-2} was obtained[19]. However, the two membranes shows poor mechanical stability and long-term durability in saline solution and under water pressure. Therefore, it is a still high challenge to fabricate membranes with high power density, mechanical stability and long-term durability.

In this study, a novel free-standing polymeric membrane is developed for robust osmotic energy generation, which is composed of thin top graphene/SPEEK layer and down PVA layer. The incorporation of ultra-thin two-dimension (2D) graphene into SPEEK thin top layer can improve the cation transportation and the mechanical properties of the composite membrane. Furthermore, the down PVA layer was prepared by a new process, providing water permeability, ion transport behavior, ion selectivity and stability. As a result, the free-standing SPEEK-G/PVA composite membrane displays exceptional mechanical stability, tunable ion flux and enhanced energy power density. This study thus opens up a new avenue for the development of membrane technologies for low-carbon and sustainable energy production.

2. Experimental

2.1 Material

PVA (1799, Macklin), PEEK (Aldrich), H_2SO_4 (98%), graphene was purchased from Chang Zhou Xi Ju Chemical Company. NaCl, KCl, ethanol (99%) and methanol (99%) were purchased from Tian Jin Damao Chemical Company.

2.2 Preparation of graphene nanosheets

The graphene was prepared by a facile two-steps method as following. Firstly, the expanded graphite (EG) was prepared by bubbling expansion method. 30g $KMnO_4$ was added to 180mL concentrated sulfuric acid in the ice bath. Natural graphite (30g) was added to above solution under mechanical stirring at room temperature for 1 h. Then,

30g Na_2CO_3 was added to above mixture under mechanical stirring. H_3PO_4 (420mL) was added into above mixed system under mechanical stirring for 5 h. Thereafter, the products were washed and filtered, forming EG. Secondly, 10g EG were added to 500mL NaOH solution (pH=14). The mixture was mechanically agitated for 2 h at 15,000 rpm using the FA 40 high shear dispersing emulsifier (Fluko), forming graphene dispersion solution. Graphene is modified with PVP and dried to give a graphene powder.

2.3 Preparation of free-standing composite membranes

The free-standing composite membranes was prepared by three-step method as shown in following Scheme 1. Firstly, sulfonated PEEK (SPEEK) was synthesized to improve the hydrophilicity of PEEK. In a 500 mL bottle flask, 5g PEEK was added to 250g H_2SO_4 (98%), and mixture was heated to 50°C. The reaction was carried out at 60°C for 12 h. The products were dropped into ice-deionized water, washed repeatedly, and freeze-dry to obtain SPEEK. 0.1g of SPEEK was dissolved in 10g methanol to obtain a solution with a mass fraction of 1 wt%. Secondly, the free-standing PVA film was prepared by molding method. A 10% PVA aqueous solution was prepared at 90°C, cooled slowly at room temperature and poured into glass dishes. The glass dishes were then transferred to a refrigerator at -20 °C for 2 h, and then thawed at room temperature for 5 h. This process was repeated 5 times to obtain the flexible, porous PVA membrane. The obtained substrate membranes were then placed in a refrigerator freezer (12 °C) and slowly dried for 5 days, followed by hot pressing at 110 °C for 2 h to obtain enhanced mechanical properties. Thirdly, PVP-modified graphene powder was dispersed in anhydrous ethanol by sonication to obtain an ethanol dispersion of graphene. The SPEEK methanol solution (1wt %) was blended with the graphene ethanol dispersion in a volume ratio of 1:1 v/v. The mixture was then ultra-sonicated for 2 h, and spin-coated onto the prepared PVA layer to afford a composite membrane with a mixed matrix top layer.

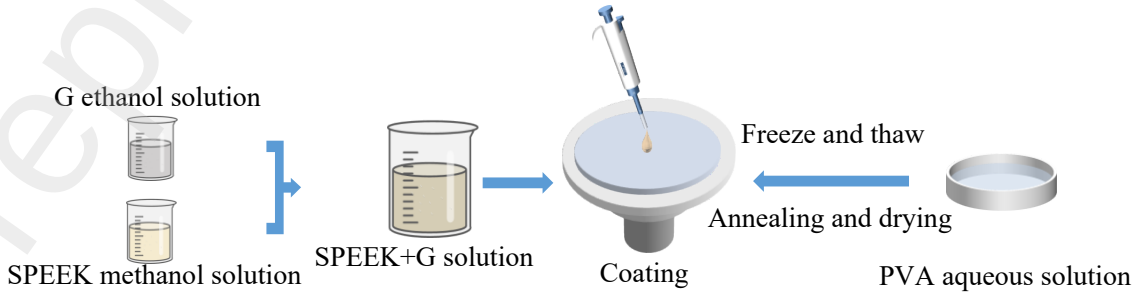

Scheme 1. The preparation of free-standing composite membranes.

2.4 Characterization

Differential scanning calorimetry (DSC) measurements were performed using the PerkinElmer DSC-7.

The ^{1}H NMR (400 MHz) analysis was conducted using a BRUKER AVANCE 400 spectrometer with DMSO-d6 as a solvent.

The FT-IR spectra were recorded on a Fourier transform infrared spectrometer (FTIR-IR-8400s)

XRD pattern was characterized by the X-ray diffractometer (XRD, Bruker).

The Raman spectra were characterized by using Laser Raman Spectrometer (Renishaw Invia).

The micro-structure of membranes were characterized by Scanning electron microscope (SEM, Hitachi SU8010).

2.5 Salinity gradient energy conversion tests

The electrochemistry measurements including I-V and osmotic energy conversion tests were carried out by using a Keithley 6487 semiconductor picoammeter (Keithley Instruments, Cleveland, OH) in a costumed device. The tested window area was 3×10^{-8} m^2 and a pair of lamellar platinum electrode was used. Asymmetric concentrations of NaCl electrolyte were added into the corresponding reservoirs. We simulated the sea water and river freshwater using 50-fold concentration gradient (0.5 M| 0.01 M NaCl).

3. Results and discussion

The ion transport process in SPEEK/G/PVA assembled membranes during osmotic energy generation is illustrated (Fig.1A).The osmotic power device is integrated by separating two reservoirs containing different concentrations of sodium chloride (NaCl) solutions with a freestanding and flexible SPEEK/G/PVA membrane in which cations are mainly allowed to pass through the ion channels in composite membranes along the salinity gradient. In addition to the ionizable sulfonic acid and carboxylic acid groups in the membrane, the ion-screening performance of the membrane also depends on the geometric channel in the membrane. The down PVA hydrogel was prepared via freeze-thaw and hot pressing methods. The resultant material exhibits hydrophilicity, high porosity, enhanced mechanical strength, making it an ideal substrate for composite membrane fabrication[20, 21]. The PEEK precursor was reacted with H_2SO_4 at elevated temperature to obtain SPEEK with pendent sulfonic acid groups along the backbone[22]. The degree of sulfonation was determined to be 60% by NMR characterization (Fig.1B). The graphene nanosheets were prepared by mechanical

exfoliation method, and characterized by AFM, TEM and Raman spectrometer (Fig.1C-E). As shown in Figure 1C and 1D, the prepared graphene are ultra-thin sheet structure with a thickness of ca.1.0nm. The Raman spectra of graphene samples show two characteristic bands of 1,325 cm^{-1} (D band) and 1,580 cm^{-1} (G band) (Fig.1E), corresponding to defective sp^3-type carbon and sp^2 hybrid aromatic carbon[23], respectively. We clearly observed the 2D band at 2,700 cm^{-1}, indicating that the aromatic structure in the stripped graphene is well preserved [24-26]. With the materials in hand, we then fabricate the SPEEK-G/PVA composite membrane to simultaneously achieve mechanical robustness and enhanced membrane performance. Specifically, SPEEK solution and graphene dispersion were mixed at a ratio of 1:1 (v/v), and the mixture was then coated onto the PVA hydrogel via spin-coating.

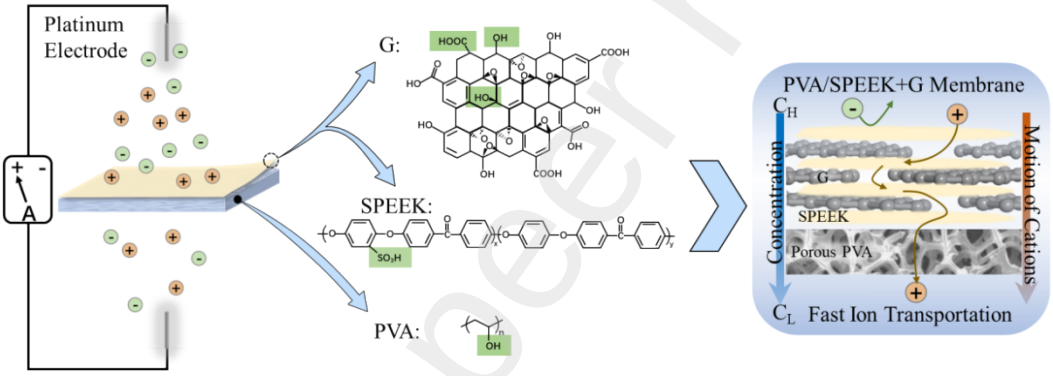

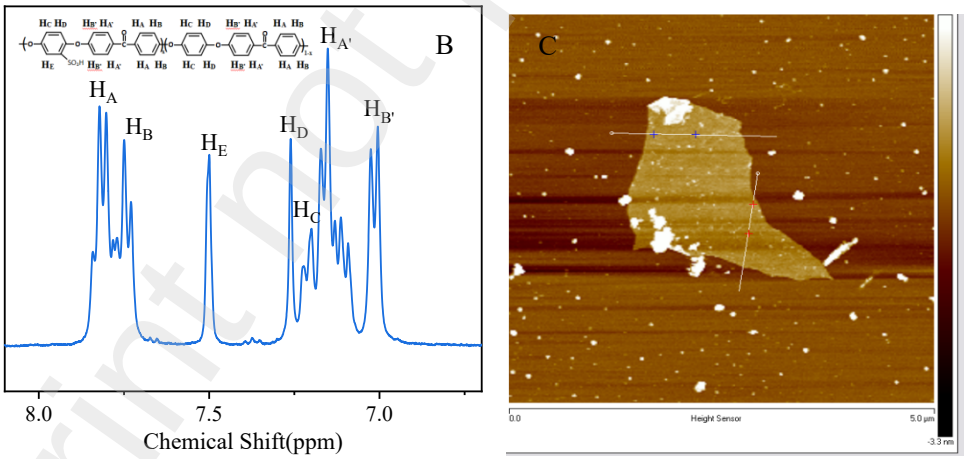

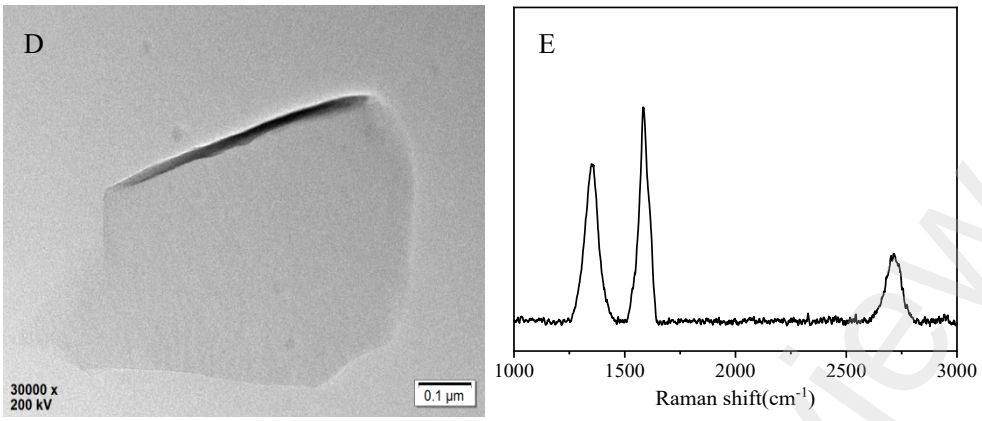

Fig.1. (A) Schematic diagram of power generation of composite membrane and composite membrane with its chemical composition, (B) ^{1}NMR analysis of SPEEK, (C) AFM image, (D) TEM image and (E) Raman spectrum of graphene nanosheets.

The successful preparation of SPEEK-G/PVA composite membrane was confirmed by the FT-IR, Raman and XRD measurements. Fig.2A shows the FT-IR spectra of PVA substrate, SPEEK precursor, SPEEK-G/PVA membrane and a control sample of SPEEK/PVA membrane. The absorption peaks at 3,320 cm^{-1} and 1,080 cm^{-1} can be assigned to O-H stretching of PVA (Fig.2A-a). The absorption peaks at 1,077cm^{-1} and 1,223cm^{-1} were assigned to the symmetric and asymmetric stretching vibrations of O=S=O groups of SPEEK, respectively (Fig.2A-b). The absorption peaks at 1,470cm^{-1} and 1,593cm^{-1} were assigned to the symmetric and asymmetric stretching vibrations of C=C groups of SPEEK, respectively. The absorption peak at 1010 cm^{-1} was assigned to S=O stretching vibrations of SPEEK. Compared to the spectrum of SPEEK/PVA membrane (Fig.2A-c), we observed two absorption peaks at 1,740cm^{-1} and 2,916 cm^{-1} from the spectrum Fig.2A-d, which can be assigned to COOH and C-H stretching vibrations of graphene, respectively. These results indicate the successful preparation SPEEK-G/PVA membrane. Fig.2B shows the Raman spectra of SPEEK-G/PVA membrane. In addition, we observed two new absorption peaks at 1,360cm^{-1} and 1,580cm^{-1}, which can be assigned to characteristic D and G bands of graphene. This result further proves the presence of graphene in SPEEK top layer. Fig.2C shows the XRD spectra of SPEEK-G/PVA composite membrane. It clearly showed two peaks at 2θ =11.7 and 19.7^{o}, which are assigned to top SPEEK-G layer and the support PVA layer, respectively. Within the top layer, the interlayer distance of nanosheets is determined to be 1.12 nm. For the PVA substrate, the peak at 2θ=19.7^{o} indicates the

formation of PVA crystalline domains, which enhance the mechanical properties of the substrate. The crystalline density of PVA layer was further determined to be 49.43% by the DSC measurement (Fig.2D)[27]. The observed smaller interlayer distance and more compact structure are expected to yield better cation transportation [28-30].

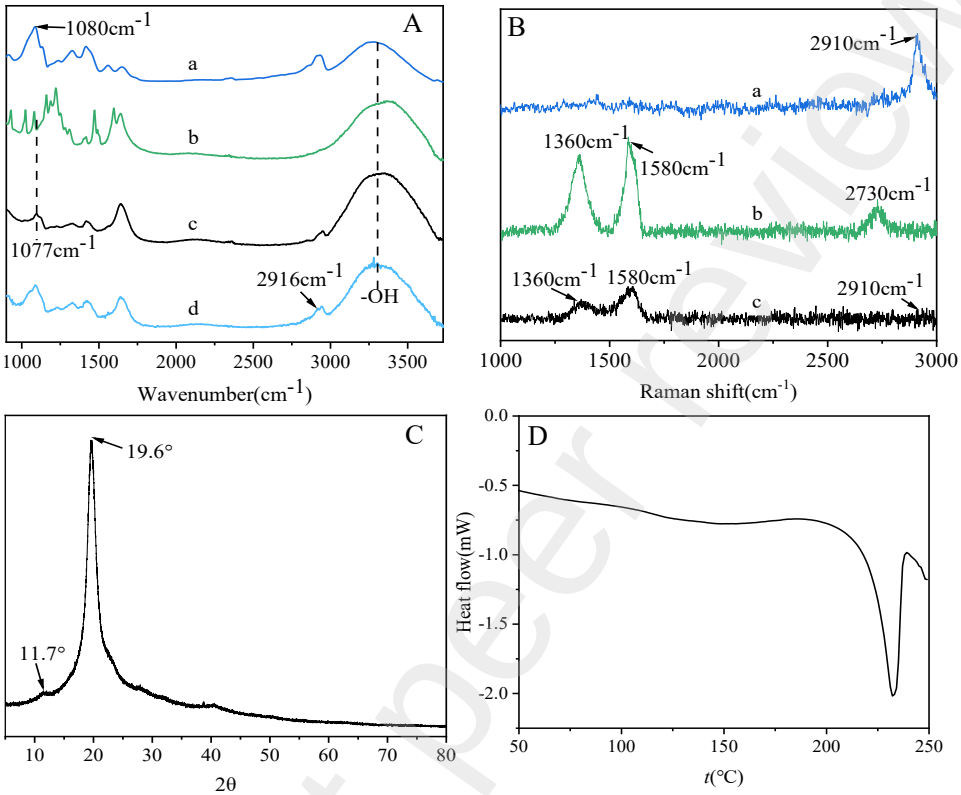

Fig.2. (A) FTIR of membranes (a, PVA. b, SPEEK. c, SPEEK/PVA. d, SPEEK-G/PVA). (B) Raman of membranes (a, PVA. b, SPEEK-G. c, SPEEK-G/PVA). (C) XRD pattern of SPEEK-G/PVA composite membrane. (D)DSC curve of PVA.

We then investigate the micro-structure of the resulting SPEEK-G/PVA membrane by SEM measurements. The incorporation of graphene nanosheets into the SPEEK matrix leads to a rough surface morphology as shown in Fig.3A. In comparison, the pure SPEEK film exhibited a smother, and more compact structure. This is because during the solvent evaporation process, the exchange rate of solvent and air in the vertical direction is different, forming a denser layer (Fig.3B). The high porosity of PVA substrate was also revealed by the SEM image shown in Fig. 3C. The cross-section SEM images revealed an asymmetric structure of the resultant SPEEK-G/PVA membrane (Fig.3D). Of particular note, the porosity and size of pores will increase in aqueous solution due to the swelling effect. As shown in Fig 4D, the total thickness of the composite membrane is *ca.* 11.8 μm with a SPEEK-G mixed matrix top layer of

380 nm. The thin thickness of top layer can significantly reduce the water and/or ions trans-membrane resistance, leading to enhanced presence. No clear boundary was observed at the interface between the top SPEEK-G layer and the PVA substrate due to their excellent compatibility. The micro-structure of SPEEK-G/PVA membrane was further characterized by AFM images (Fig.3E-F). The Ra and Rq values of PVA were 4.1 and 5.5nm, the Ra and Rq of SPEEK-G were 10.1 and 12.8nm, respectively. For SPEEK-G, the dark regions represent the hydrophilic domains formed by the aggregation of sulfonated SPEEK segments. These domains form transport channels for water molecules and cations as well as selectivity for anions.

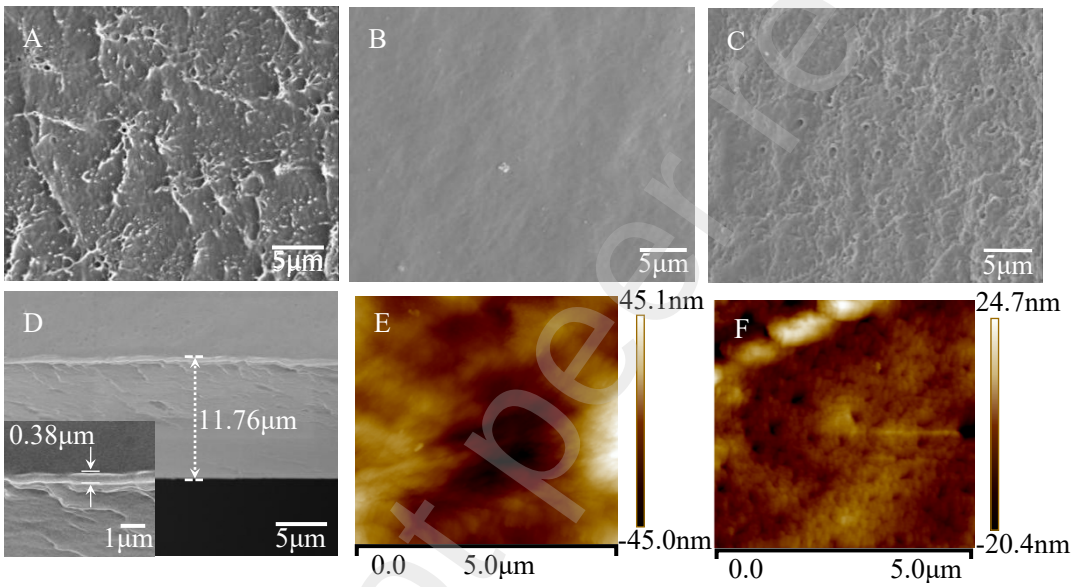

Fig.3. SEM images of (A) top SPEEK-G layer, (B) top SPEEK layer and (C) support PVA layer. (D) SEM images of Cross-section SPEEK-G/PVA composite membrane. AFM images of (E) SPEEK-G layer and (F) PVA layer.

We finally evaluated the membrane performance using a costumed osmotic energy generation device. (Fig.4A). The osmotic power device is integrated by separating two reservoirs containing different concentrations of sodium chloride (NaCl) solutions with a freestanding and flexible SPEEK-G/PVA membrane, in which cations are allowed to pass through the ion channels in composite membranes along the salinity gradient. In addition to the ionizable sulfonic acid (of SPEEK) and carboxylic acid groups (of G-nanosheets) in the membrane, the ion-screening performance of the membrane also depends on the geometric channel in the membrane. The ion transport behaviors of SPEEK/PVA or SPEEK-G/PVA composite membranes were characterized and compared by the ionic current-voltage (I-V) property first. The linear ohmic ion

transport behavior over a range of NaCl electrolyte concentrations indicates the asymmetric structure of the composite membrane (Fig.4B). The ionic conductance over a series of NaCl concentrations is plotted as a function of electrolyte concentration (Fig.4C). This result reveals the obvious charge-governed ion transport and confined ion transport behaviors through the SPEEK/PVA or SPEEK-G/PVA composite membrane. There is a critical concentration point at approximately 0.01 M electrolyte. Above this point, the ionic conductance follows the bulk rule of linearly increasing with concentration due to the thin electrical double layer (EDL)[17, 31]. However, as the concentration decreases to the critical point, a strong nonlinear relationship is observed, and the ionic conductivity deviates sharply from the bulk value, reaching a plateau. This interesting phenomenon induced by the overlapping EDL in the ion transport channels results in ion enrichment in the confined spaces, where the ion transport behavior is determined by the surface and space charges of the SPEEK/PVA or SPEEK-G/PVA composite membranes, rather than determined by the bulk concentration[4, 32]. Fig.4D shows variation of different current densities with increasing load resistance for the SPEEK/PVA or SPEEK-G/PVA composite membranes. The diffusion current gradually decreased with the increase of load resistance, and the output power density reached its peak value when the load resistance was approximately 20kΩ (Fig.4E). Compared with PVA or SPEEK/PVA membranes, the SPEEK-G/PVA composite membrane showed a low resistance of 20kΩ (Fig.4E) and a higher current density (Fig.4D), leading to a high output power density. The maximal power densities of different membranes were concluded in Fig.4F. Compared with PVA (ca.2.0W/m^2) or SPEEK/PVA membranes (ca.5.2W/m^2), the SPEEK-G/PVA composite membrane exhibited the highest power density of 5.89W/m^2. This is achieved by creating interfacial voids between the graphene flakes and SPEEK chains (due to the repulsion between $-COO^-$ and $-SO_3^-$ groups), which increases the fractional free volume within the top layer, thereby increasing the permeation rate[33].

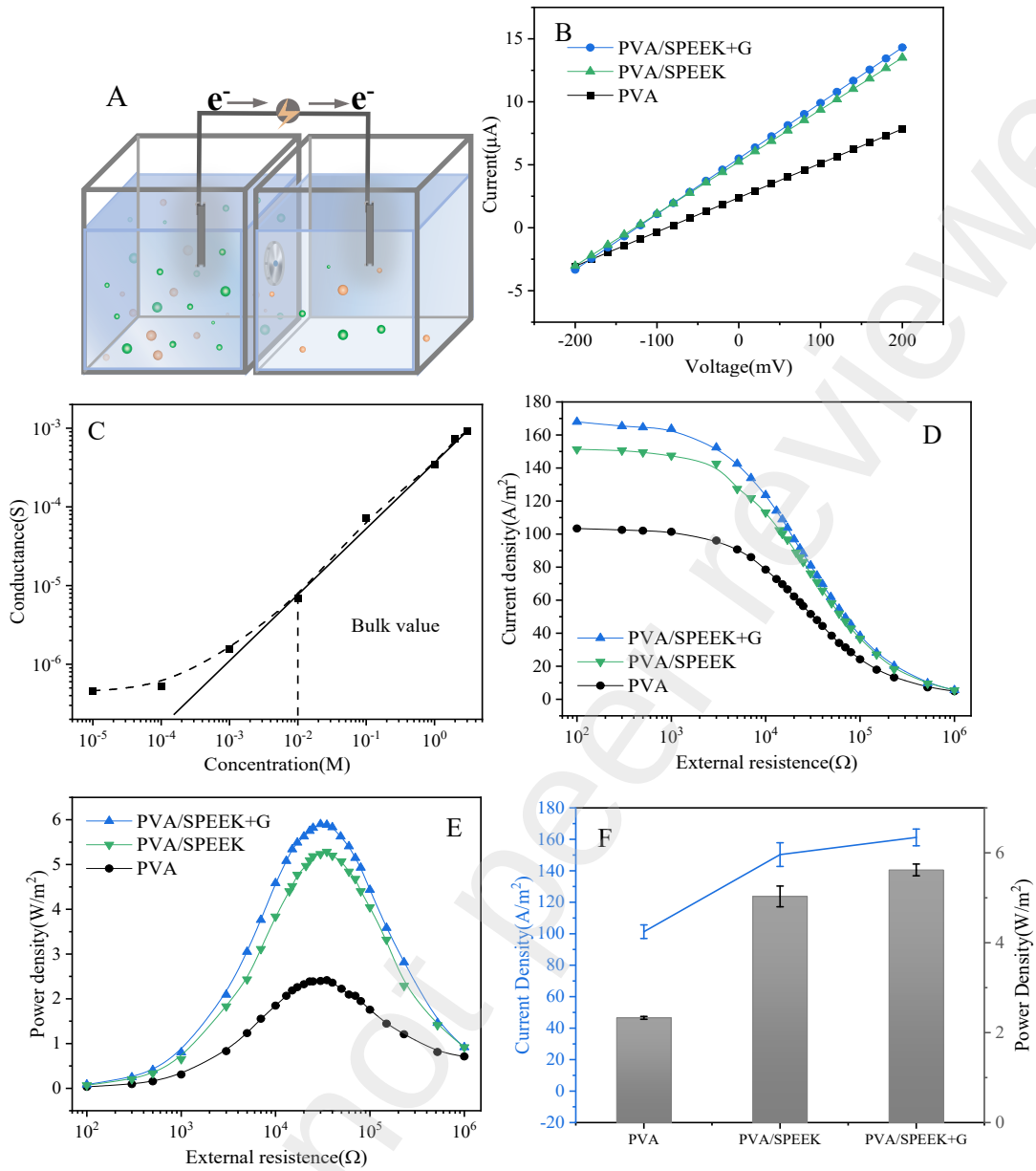

Fig.4. (A) Diagram of osmotic energy generation device. (B) I-V curves of PVA, SPEEK/PVA membranes and SPEEK-G/PVA composite membrane under two configured NaCl concentration gradients. (C) Ionic conductance in a range of concentrations of neutral NaCl electrolyte. (D) The current density and (E) power density of PVA, SPEEK/PVA membranes and SPEEK-G/PVA composite membrane as a function of load resistance. (F) The Maximal current density and power density of various membranes.

In order to optimize the configuration, a 500-fold concentration gradient (5 M/0.01 M NaCl) was adopted and the result was shown in Fig.5A. The power density increased from 5.8 to 20.3W/m^2 for the SPEEK-G/PVA. From Fig.5B, we can conclude that both negative and positive ionic currents are relatively constant, and each cycle can last for

50 s and repeated 7 times. In addition, we performed a 96-h energy collection test using the constructed membrane-based generator. As seen from Fig.5C, the obtained current remained stable during long-term testing. These results confirm the excellent chemical stability and long-term durability of SPEEK-G/PVA heterogeneous composite membrane.

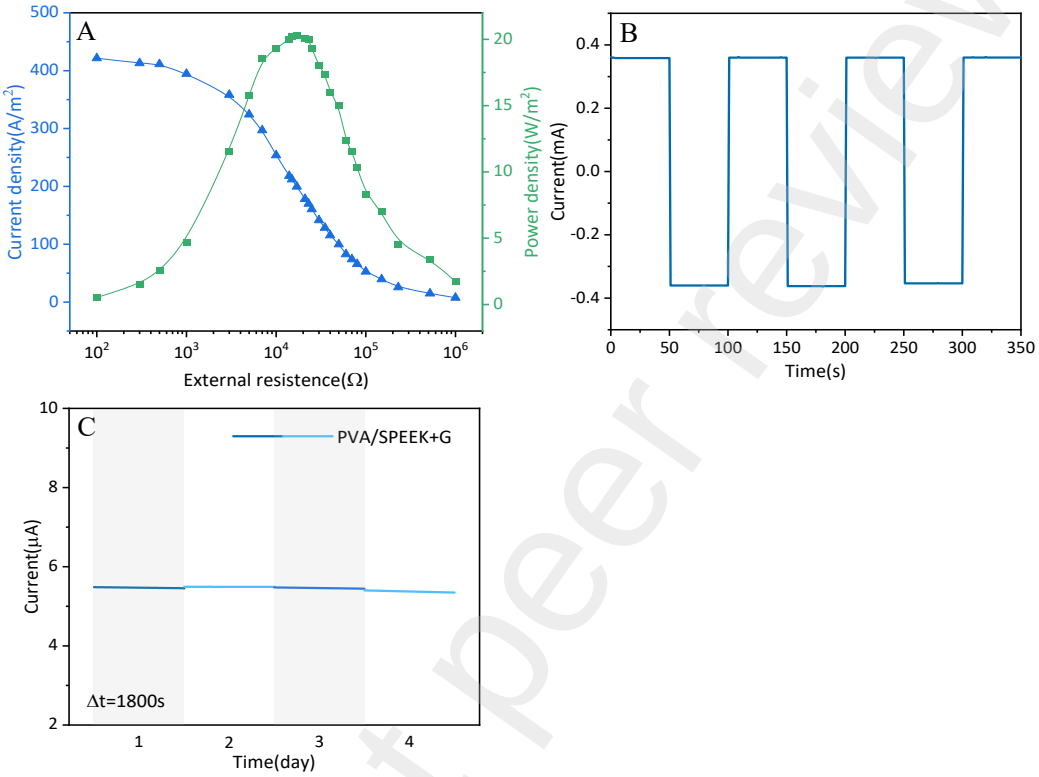

Fig.5. (A) Power density and Current density of membranes at a gradient of 500. (B) The ionic current curve of the membrane with an alternately external bias of +2V/-2 V shows its stable ion transport property. (C) Long-term stability of the membrane-based generator.

The mechanical stability of the SPEEK-G/PVA composite membrane was further characterized by using a self-made setup (Fig.6A). A pressure (*P*, Pa) was applied to the membrane, which was determined by Eq 1:

$$P = \rho g h \quad (1)$$

where ρ (g/cm^3), g (9.8N) and h (cm) are the density of water, gravity and height of air, respectively. Here, the pressure applied to the composite membrane was calculated to be 300 Pa. We observed that the SPEEK-G/PVA membrane can maintain its integrity under this pressure. The water is forced through these membranes by applied pressure. Interestingly, water is not absorbed by the membrane like other PVA-based hydrophilic membranes. The result may be attributed to the high degree of crystallinity of PVA

substrate[34]. The SPEEK-G/PVA membrane shows a high water flux rate of 0.51 L/m^2 h due to its high hydrophilicity, thin top layer and porous substrate (Fig.6B). For osmotic energy generation device, higher flux rate are highly desirable to improve ions transportation rates, increase current and power densities, and reduce fouling. The output power density and current density of SPEEK-G/PVA composite membrane after pressure treatment were characterized as a function of load resistances (Fig.6C). The diffusion current gradually decreased with the increase of load resistance, and the output power density reached its peak value when the load resistance was approximately 23kΩ. The maximum power density was calculated to be 5.7W/m^2, which is identical to the value before pressure treatment. These results further prove the enhanced mechanical stability of the SPEEK-G/PVA membrane.

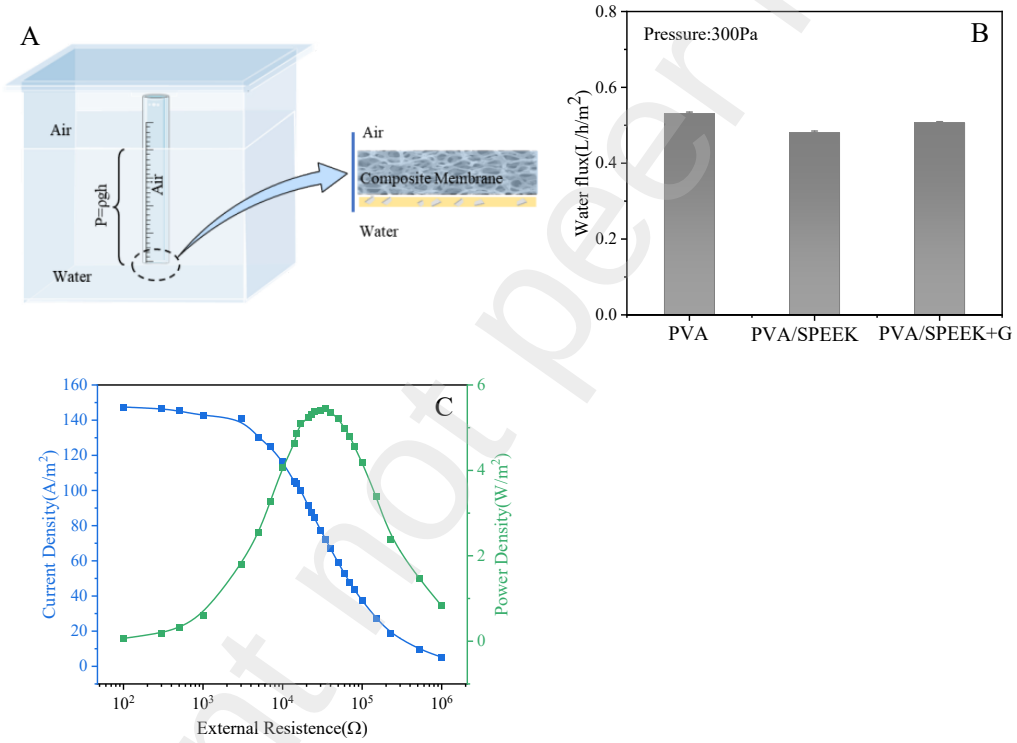

Fig.6. (A) Schematic diagram of Pressure experiment. (B) Water flux of the membrane at 300Pa pressure. (C) Power density and Current density of composite membranes after Pressure experiment with a gradient of 50.

4. Conclusions

In this study, we have successfully fabricated a composite membrane containing graphene nanosheets in its top layer. Benefiting from the asymmetry in chemical composition and membrane configuration, the ions transport could be boosted and regulated as required. High performance of osmotic energy generation is attributed to

the successful incorporation of nanosheets, which is favorable for ion transport. Moreover, as nanofillers, the addition of graphene nanosheets further enhances the mechanical properties of the resulting composite membrane. Our work thus opens up a new avenue for the development of membrane-based technology for practical energy generation applications.

Acknowledgments

Financial support from Shanxi Provincial Natural Science Foundation (202104021301059, YDZJSX2021A026).

References

[1] Bandh S A, Shafi S, Peerzada M, Rehman T, Bashir S, Wani S A, Dar R. Multidimensional analysis of global climate change: a review [J]. Environ Sci Pollut Res Int, 2021, 28(20): 24872-24888.

[2] Chen N, Lee Y M. Anion exchange polyelectrolytes for membranes and ionomers [J]. Progress in Polymer Science, 2021, 113(24): 101345-101380.

[3] Olsson M, Wick G L, Isaacs J D. Salinity gradient power: utilizing vapor pressure differences [J]. Science, 1979, 206(4417): 452-454.

[4] Lin X, Liu P, Xin W, Teng Y, Chen J, Wu Y, Zhao Y, Kong X Y, Jiang L, Wen L. Heterogeneous MXene/PS-b-P2VP Nanofluidic Membranes with Controllable Ion Transport for Osmotic Energy Conversion [J]. Advanced Functional Materials, 2021, 31(45): 2105013-2105023.

[5] Sheng N, Zhang M, Song Q, Zhang H, Chen S, Wang H, Zhang K. Enhanced salinity gradient energy harvesting with oppositely charged bacterial cellulose-based composite membranes [J]. Nano Energy, 2022, 101(12): 107548-107557.

[6] Zhang Z, Wen L, Jiang L. Nanofluidics for osmotic energy conversion [J]. Nature Reviews Materials, 2021, 6(7): 622-639.

[7] Xu Y, Zhang K, Chen S, Zhang X, Chen Y, Li D, Xu F. Two-dimensional lamellar MXene/three-dimensional network bacterial nanocellulose nanofiber composite Janus membranes as nanofluidic osmotic power generators [J]. Electrochimica Acta, 2022, 412(6): 140162-140169.

[8] Q. Liu, Z.T. Tang, Z.G. Qu, Qinlong Ren, J.F. Zhang, R.X. Tang, A capacitor-based power equivalent model for salinity-gradient osmotic energy conversion, Energy Conversion and Management, 2021, 250:114862

[9] Zhang Z, He L, Zhu C, Qian Y, Wen L, Jiang L. Improved osmotic energy conversion in heterogeneous membrane boosted by three-dimensional hydrogel

interface [J]. Nat Commun, 2020, 11(1): 875-883.
[10] Wang C, Liu F F, Tan Z, Chen Y M, Hu W C, Xia X H. Fabrication of Bio-Inspired 2D MOFs/PAA Hybrid Membrane for Asymmetric Ion Transport [J]. Advanced Functional Materials, 2019, 30(9): 1908804-1908814.
[11] Sui X, Zhang Z, Li C, Gao L, Zhao Y, Yang L, Wen L, Jiang L. Engineered Nanochannel Membranes with Diode-like Behavior for Energy Conversion over a Wide pH Range [J]. ACS Appl Mater Interfaces, 2019, 11(27): 23815-23821.
[12] Zhou S, Xie L, Li X, Huang Y, Zhang L, Liang Q, Yan M, Zeng J, Qiu B, Liu T, Tang J, Wen L, Jiang L, Kong B. Interfacial Super-Assembly of Ordered Mesoporous Carbon-Silica/AAO Hybrid Membrane with Enhanced Permselectivity for Temperature- and pH-Sensitive Smart Ion Transport [J]. Angew Chem Int Ed Engl, 2021, 60(50): 26167-26176.
[13] Stein D, Kruithof M, Dekker C. Surface-charge-governed ion transport in nanofluidic channels [J]. Phys Rev Lett, 2004, 93(3): 35901-35904.
[14] Fan R, Huh S, Yan R, Arnold J, Yang P. Gated proton transport in aligned mesoporous silica films [J]. Nat Mater, 2008, 7(4): 303-307.
[15] Zhang Z, Kong X Y, Xiao K, Liu Q, Xie G, Li P, Ma J, Tian Y, Wen L, Jiang L. Engineered Asymmetric Heterogeneous Membrane: A Concentration-Gradient-Driven Energy Harvesting Device [J]. J Am Chem Soc, 2015, 137(46): 14765-14772.
[16] Xu Y, Song Y, Xu F. TEMPO oxidized cellulose nanofibers-based heterogenous membrane employed for concentration-gradient-driven energy harvesting [J]. Nano Energy, 2021, 79(20): 105468-105495.
[17] Zhang Z, Yang S, Zhang P, Zhang J, Chen G, Feng X. Mechanically strong MXene/Kevlar nanofiber composite membranes as high-performance nanofluidic osmotic power generators [J]. Nat Commun, 2019, 10(1): 2920-2929.
[18] Wu Y, Xin W, Kong X-Y, Chen J, Qian Y, Sun Y, Zhao X, Chen W, Jiang L, Wen L. Enhanced ion transport by graphene oxide/cellulose nanofibers assembled membranes for high-performance osmotic energy harvesting [J]. Materials Horizons, 2020, 7(10): 2702-2709.
[19] Zhao X, Lu C, Yang L, Chen W, Xin W, Kong X-Y, Fu Q, Wen L, Qiao G, Jiang L. Metal organic framework enhanced SPEEK/SPSF heterogeneous membrane for ion transport and energy conversion [J]. Nano Energy, 2021, 81(24): 105657-105666.
[20] Ellison. T M, Spencer. H G. ELECTROCHEMICAL PROPERTIES OF IONOGENIC MEMBRANES PREPARED BY THERMAL AND OXIDATIVE

401 DEGRADATION OF POLY(VINYL ALCOHOL) [J]. POLYMER LETTERS, 1963,
402 1(11): 707-710.
403 [21]SPENCER. H G, HUN. O L. Electrochemistry of Poly (Methyl Vinyl Ether-Maleic
404 Anhydride)-Polyvinyl Alcohol Membranes [J]. JOURNAL OF APPLIED POLYMER
405 SCIENCE, 1962, 6(24): 656-658.
406 [22]Kim A R, Vinothkannan M, Yoo D J. Sulfonated-fluorinated copolymer blending
407 membranes containing SPEEK for use as the electrolyte in polymer electrolyte fuel
408 cells (PEFC) [J]. International Journal of Hydrogen Energy, 2017, 42(7): 4349-4365.
409 [23]Tang H, He P, Huang T, Cao Z, Zhang P, Wang G, Wang X, Ding G, Xie X.
410 Electrochemical method for large size and few-layered water-dispersible graphene [J].
411 Carbon, 2019, 143(22): 559-563.
412 [24]Xiong Z, Liao C, Han W, Wang X. Mechanically Tough Large-Area Hierarchical
413 Porous Graphene Films for High-Performance Flexible Supercapacitor Applications [J].
414 Adv Mater, 2015, 27(30): 4469-4475.
415 [25]Chen H, Qi C, Shen L, Fu Q, Wang Z, Xiong Z, Sun Y, Liu Y. Tunable d-spacing
416 of dry reduced graphene oxide nanosheets for enhancing re-dispersibility in organic
417 solvents [J]. Applied Surface Science, 2020, 531(14): 147375-147384.
418 [26]Xiong Z, Yun X, Qiu L, Sun Y, Tang B, He Z, Xiao J, Chung D, Ng T W, Yan H,
419 Zhang R, Wang X, Li D. A Dynamic Graphene Oxide Network Enables Spray Printing
420 of Colloidal Gels for High-Performance Micro-Supercapacitors [J]. Adv Mater, 2019,
421 31(16): 1804434-1804441.
422 [27]Meo O, Ngui S K, Mallapragada. Understanding isothermal semicrystalline
423 polymer drying: Mathematical models and experimental characterization [J]. Journal of
424 Polymer Science: Part B: Polymer Physics, 1998, 36(15): 2771-2780.
425 [28]Alia S H, Nikolaos A P. Mesh size and diffusive characteristics of semicrystalline
426 poly(vinyl alcohol) membranes prepared by freezing/thawing techniques [J]. Journal of
427 Membrane Science, 1995, 107(9): 229-237.
428 [29]Amanda. A, Kulprathipanja. A, Toennesen. M, Mallapragada. S K. Semicrystalline
429 poly(vinyl alcohol) ultrafiltration membranes for bioseparations [J]. Journal of
430 Membrane Science, 2000, 176(8): 87-95.
431 [30]PEPPAS. N A, MERRILL. E W. Poly(viny1 Alcohol) Hydrogels: Reinforcement
432 of Radiation-Crosslinked Networks by Crystallization [J]. JOURNAL OF POLYMER
433 SCIENCE: Polymer Chemistry Edition, 1976, 14:441-457.
434 [31]Ji J, Kang Q, Zhou Y, Feng Y, Chen X, Yuan J, Guo W, Wei Y, Jiang L. Osmotic

Power Generation with Positively and Negatively Charged 2D Nanofluidic Membrane Pairs [J]. Advanced Functional Materials, 2017, 27(2): 1603623-1603631.

[32]Jia P, Du X, Chen R, Zhou J, Agostini M, Sun J, Xiao L. The Combination of 2D Layered Graphene Oxide and 3D Porous Cellulose Heterogeneous Membranes for Nanofluidic Osmotic Power Generation [J]. Molecules, 2021, 26(17):5343-5354.

[33]Berean K J, Ou J Z, Nour M, Field M R, Alsaif M M Y A, Wang Y, Ramanathan R, Bansal V, Kentish S, Doherty C M, Hill A J, McSweeney C, Kaner R B, Kalantar-zadeh K. Enhanced Gas Permeation through Graphene Nanocomposites [J]. The Journal of Physical Chemistry C, 2015, 119(24): 13700-13712.

[34]NIKOLAOS A P, EDWARD W M. Poly(vinyl Alcohol) Hydrogels: Reinforcement of Radiation-Crosslinked Networks by Crystallization [J]. JOURNAL OF POLYMER SCIENCE: Polymer Chemistry Edition, 1976, 14(4): 441-457.